

Video Article

Vasodilation of Isolated Vessels and the Isolation of the Extracellular Matrix of Tight-skin Mice

Dorothee Weihrauch¹, John G. Krolikowski^{1,2}, Deron W. Jones³, Tahniyath Zaman³, Omoshalewa Bamkole¹, Janine Struve⁴, Paul S. Pagel⁵, Nicole L. Lohr⁶, Kirkwood A. Pritchard, Jr.³

¹Department of Anesthesiology, Medical College of Wisconsin

²Clement J. Zablocki Veterans Affairs Medical Center

³Department of Surgery, Division of Pediatric Surgery, Children's Research Institute

⁴Department of Orthopedic Surgery, Medical College of Wisconsin

⁵Department of Anesthesiology, Clement J. Zablocki Veteran Affairs Medical Center

⁶Department of Medicine, Division of Cardiology, Medical College of Wisconsin

Correspondence to: Dorothee Weihrauch at dorothee@mcw.edu

URL: <https://www.jove.com/video/55036>

DOI: [doi:10.3791/55036](https://doi.org/10.3791/55036)

Keywords: Immunology, Issue 121, inflammation, fibrosis, myocardium, endothelial function, IRF5, scleroderma

Date Published: 3/24/2017

Citation: Weihrauch, D., Krolikowski, J.G., Jones, D.W., Zaman, T., Bamkole, O., Struve, J., Pagel, P.S., Lohr, N.L., Pritchard, Jr., K.A. Vasodilation of Isolated Vessels and the Isolation of the Extracellular Matrix of Tight-skin Mice. *J. Vis. Exp.* (121), e55036, doi:10.3791/55036 (2017).

Abstract

The interferon regulatory factor 5 (IRF5) is crucial for cells to determine if they respond in a pro-inflammatory or anti-inflammatory fashion. IRF5's ability to switch cells from one pathway to another is highly attractive as a therapeutic target. We designed a decoy peptide IRF5D with a molecular modeling software for designing small molecules and peptides.

IRF5D inhibited IRF5, reduced alterations in extracellular matrix, and improved endothelial vasodilation in the tight-skin mouse (Tsk/+). The K_d of IRF5D for recombinant IRF5 is $3.72 \pm 0.74 \times 10^{-6}$ M as determined by binding experiments using biolayer interferometry experiments. Endothelial cells (EC) proliferation and apoptosis were unchanged using increasing concentrations of IRF5D (0 to 100 μ g/mL, 24 h). Tsk/+ mice were treated with IRF5D (1 mg/kg/d subcutaneously, 21 d). IRF5 and ICAM expressions were decreased after IRF5D treatment. Endothelial function was improved as assessed by vasodilation of facialis arteries from Tsk/+ mice treated with IRF5D compared to Tsk/+ mice without IRF5D treatment. As a transcription factor, IRF5 traffics from the cytosol to the nucleus. Translocation was assessed by immunohistochemistry on cardiac myocytes cultured on the different cardiac extracellular matrices. IRF5D treatment of the Tsk/+ mouse resulted in a reduced number of IRF5 positive nuclei in comparison to the animals without IRF5D treatment (50 μ g/mL, 24 h). These findings demonstrate the important role that IRF5 plays in inflammation and fibrosis in Tsk/+ mice.

Video Link

The video component of this article can be found at <https://www.jove.com/video/55036/>

Introduction

Regulation of cell growth and cell death immune responses is central to the role of the transcription factor family of interferon regulatory factors. IRF5 is highlighted as being crucial for the regulation of immune responses between type 1, an inflammatory promoting response and type 2, an immune response targeting tissue repair. IRF5 is key in cancer¹, and autoimmunity^{2,3,4,5}.

The tight-skin mouse (Tsk/+) is a model for tissue fibrosis and scleroderma due to a duplication mutation in the fibrillin-1 gene. This mutation results in a tight-skin and an increase in connective tissue. These mice develop myocardial inflammation, fibrosis and finally heart failure^{5,6,7,8,9}. Scleroderma is an autoimmune fibrotic disorder affecting approximately 150,000 patients in the United States⁶. The hallmarks of this disease are fibrosis of internal organs including the heart^{7,8,9,10,11}.

The nature of the study demanded the design of an inhibitory peptide. The software approach was chosen over a traditional approach using a phage display. The software approach is easier and less time consuming. The RCSB data bank is used to identify appropriate binding sites¹². To study the interaction of the newly designed peptide with the recombinant protein and to focus on the binding parameters, a technique called biolayer interferometry was used. Biolayer interferometry is a biosensor based technique that determines binding affinity, association and disassociation using a biosensor and a binding sample. The biosensor can be fluorescently, luminescently, radiometrically and colorimetrically labeled. The measurement is based on mass addition or depletion resembling association and disassociation^{13,14}. The aim of this study was to understand the role of IRF5 in myocardial inflammation and fibrosis. The goal was to gain insight into the role of IRF5 in the development of tissue fibrosis and scleroderma.

Protocol

This study was carried out in strict accordance with the recommendations in the Guide for the Care and Use of Laboratory Animals of the National Institutes of Health. The protocol was approved by the Institutional Animal Care and Use Committee (Protocol: AUA#1517). All research involving mice was conducted in conformity with PHS policy.

1. Design of Decoy Peptide

1. Find the IRF5's 3D structure and base the design on it. Design a 17 mer, termed IRF5D (ELDWDADDIRLQIDNPD), where aspartate (D) is substituted for serine (S) to mimic phosphorylation in IRF5 at 421 - 438 (ELSWADSIRLQISNPD). Analysis of 3D sulfhydryl groups and knowledge of IRF5's mechanism of activation, *i.e.*, serine phosphorylation, suggested that one strategy for targeting IRF5 was to generate a decoy peptide. See **Figure 1**. To identify the best region in the 3D structure, use a molecular modeling software for designing small molecules and peptides¹⁵.

NOTE: The critical step in this process is the availability of the 3D structure of the target protein and its possible binding sites. The 3D structure of IRF5 accurately represents how IRF5 dimerizes after phosphorylation. The substitution of aspartate for serine or threonine is outsourced. The peptide is synthesized separately without being linked to IRF5.

2. Replicate the phospho-domain simply by substituting D for S. Based on the original sequence (ELSWADSIRLQISNPD), make a new peptide IRF5S with the amino acid sequence of Ac-ELDWDADDIRLQIDNPD-NH₂ (IRF5D).

2. Biolayer Interferometry (BLI)

NOTE: The purification for recombinant IRF5 was outsourced.¹⁶

1. Biotin label IRF5 in a molar ratio of 1:1 of biotin to ligand with a biotinylation reagent incorporating a long-chain linker. The long chain linker will ensure a more active and homogenous ligand surface.
 1. Add 1 mL of 2 mg/mL IRF5 to 13 μ L of 20 mM biotin reagent or increase the volumes if needed. Incubate on ice for 2 h. After labeling, use a desalting spin column to remove the reaction mixture from the labeled protein.
2. Incubate the biotin-labeled ligand with the biosensors for 15 min. Avoid over-labeling and adjust the 1:1 molar ratio. After labeling, use a desalting spin column to remove the reaction mixture from the labeled protein.
3. Incubate the biotin labeled IRF5 biosensors for 10 min in different concentrations of the IRF5 decoy peptide. The association and dissociation rates were determined as described^{10,17,18}.

3. Apoptosis and Proliferation Assays

1. Proliferation assay via bioreduction of the tetrazolium

1. Administer IRF5D diluted in PBS (1 mg/kg/d, inject a volume 20 μ L in a 20 g mouse) subcutaneously with a 27-gauge needle by a standard scruffing technique or by PBS alone to Tsk/+ and C57Bl/6J mice for 21 days.
2. Anesthetize the mice with isoflurane (5%) and perform a cervical dislocation. Excise the hearts by cutting open the chest along the sternum. Lift up the heart with forceps and remove the heart.
3. Lyse the hearts with a protein lysis buffer containing 50 mM Tris-HCl pH 7.4, 0.5% NP-40, 250 mM NaCl, 5 mM EDTA, 50 mM NaF¹⁰ and determine protein concentration by Bradford assay¹⁹.
4. Coat 96-well plates with C57Bl/6J cardiac matrix isolated as described in section 7. Dilute the PBS suspended C57Bl/6J cardiac matrix to a concentration of 20 μ g/mL and add 30 μ L of the C57Bl/6J cardiac to each well. Let it settle overnight at 37 °C in the incubator.
5. Culture human umbilical vein cells using 500 mL of endothelial basal media with 0.4% bovine brain extract, 0.1% ascorbic acid, 0.1% hydrocortisone, 0.1% human epidermal growth factor, 2% fetal bovine serum and 0.1% gentamicin/amphotericin B added to it. Culture the cells on 96 well plates at 5% CO₂ and 95% room air with a density of 25,000 cells per well. Stimulate with increasing concentrations of IRF5D between 0 - 100 μ g/mL into the media (volumes were between 0 and 50 μ L/mL).
6. Determine the cell proliferation after three days and assess differences in absorbance on a microplate reader. The reaction is a bioreduction of MTS tetrazolium compound. NADPH or NADH is produced by dehydrogenase enzymes in metabolically active cells.
7. As the MTS tetrazolium compound is stored frozen at -20 °C, thaw the compound slowly over approximately 90 minutes at room temperature. Pipette 20 μ L into each well of a 96 well plate, and add 100 μ L of culture media to it. Incubate plate at 37 °C for 1 to 4 h in a humidified, 5% CO₂ chamber.
8. Read absorbance at a wavelength of 490 nm.

2. Apoptosis assay via caspase activity

NOTE: The experimental set-up is the same as above 3.1.1 to 3.1.5.

1. Stimulate the cells with increasing concentrations of IRF5D between 0 - 100 μ g/mL into the media.
2. Add green detection to the Caspase 3/7 substrate to the ECs and incubate it for 30 min at 37 °C. Assess the fluorescence on the microplate reader simultaneously with an absorption/emission wavelength of 502/530 nm. Run the experiments in triplicate.

NOTE: The green fluorescent agent is a four amino acid peptide bound to a nucleic acid binding dye. This reagent becomes fluorescent when cleaved after caspase 3 and 7 activation. This fluorescence is measured. The advantage is a reduction in wash steps.

4. Assessment of the IRF5 and ICAM-1 Expression in the Heart

1. Administer IRF5D diluted in PBS (1 mg/kg/d, inject a volume 20 μ L in a 20 g mouse) subcutaneously with a 27-gauge needle by a standard scruffing technique or by PBS alone to Tsk/+ and C57Bl/6J mice once per day for 21 days.
2. Anesthetize the mice with isoflurane (5%) and perform a cervical dislocation. Excise the hearts by cutting open the chest along the sternum. Lift up the heart with forceps and remove the heart.
3. Lyse the hearts with a protein lysis buffer containing 50 mM Tris-HCl pH 7.4, 0.5% NP-40, 250 mM NaCl, 5 mM EDTA, 50 mM NaF¹⁰ and determine protein concentration by Bradford assay¹⁹.
 1. Perform a western blot on lysates of hearts. Dilute the samples to 25 μ g total protein and a volume of 40 μ L with Laemmli sample buffer containing 5% mercaptoethanol. Run the samples on a 4 - 15% TGX gel at 50 mV for 5 min. Increase voltage to 100 mV for 1 h until the dye front runs out.
 2. Place the gel in 1x transfer buffer (25 mM Tris, 190 mM glycine, 20% methanol, adjust pH to 8.3 if necessary) and incubate for 10 - 15 min.
 3. Assemble the transfer sandwich (sponge, filter, gel, cellulose membrane, filter, sponge). Make sure no bubbles are trapped in between. The blot should be on the cathode and the gel on the anode. Transfer for 1 h in the cold room at 100 mA.
 4. The next day, rinse the blot and then block the background in 5% nonfat dry milk for 30 min at room temperature. Rinse the blot with Tris buffered saline containing 5% Tween three times for 5 min each.
 5. Incubate overnight with the primary antibodies using primary polyclonal antibodies to IRF5 or ICAM-1. Dilute the antibodies in Tris buffered saline in a 1:1,000 dilution.
 6. Dilute the secondary antibodies in Tris buffered saline and incubate the blot for 1 h at room temperature. For secondary antibodies, use horseradish peroxidase conjugated donkey anti-mouse IgG (1:10,000) and horseradish peroxidase donkey anti-goat IgG (1:10,000), respectively.
 7. Apply chemiluminescence to the blot after mixing components according to manufacturer's protocol and incubate for 3 min to luminesce the bands of interest. Expose the blot to an X-ray film. Use ImageJ to measure density. Normalize the density values to the control bands¹⁰.

5. Assessment of Inflammatory Cell Numbers after IRF5 Inhibition

1. Administer IRF5D diluted in PBS (1 mg/kg/d) subcutaneously with a 27-gauge needle by a standard scruffing technique or by PBS alone to Tsk/+ and C57Bl/6J mice for 21 days.
2. Anesthetize the mice with isoflurane (5%) and perform a cervical dislocation. Excise the hearts by cutting open the chest along the sternum. Lift up the heart with forceps and remove the heart. Snap freeze and store the excised hearts until analysis.
3. Mount the frozen hearts on tissue holders appropriate to the cryostat in use. Cut 10 μ m thick frozen sections on a cryostat for immunohistochemistry.
4. Fix the frozen sections with 1% paraformaldehyde in phosphate buffered saline for 20 min at room temperature. Permeabilize the sections with 0.5% Triton-X 100 in PBS for 5 min.
Caution: Paraformaldehyde is a regulated carcinogen and needs to be handled with care.
5. Dilute anti-rabbit CD64, a monocyte/macrophage marker 1:200 in PBS. Apply to the fixed sections and incubate for 30 min at 37 $^{\circ}$ C.
6. Wash slides in PBS for 5 min three times at room temperature.
7. Dilute anti-rat NIMP, a primary neutrophil marker 1:200 in PBS. Apply to the fixed sections and incubate for 30 min at 37 $^{\circ}$ C.
8. Wash the slides for 5 min three times with PBS at room temperature.
9. Dilute the secondary antibodies anti-rabbit Alexa 488 conjugated and anti-rat Alexa 488 conjugated 1:200 in PBS.
10. Apply anti-rabbit Alexa 488 conjugated and anti-rat Alexa 488 conjugated secondary antibodies to the sections for 30 min at 37 $^{\circ}$ C accordingly. The volume of antibody varies according to the size of the section. The amount should cover the section generously. In most cases the volume is between 100 and 200 μ L.
11. Use 4',6-diamidino-2-phenylindole (DAPI) as a nuclear stain in a 1:1,000 dilution in PBS. Add 1 μ L into 1 mL PBS and use the DAPI in the last wash step. Add aqueous mounting media to a cover slip and put it onto the slide.
12. Analyze the fluorescently labeled sections by confocal microscopy using a 40X oil objective. Use excitation wavelengths 488 and emission wavelengths of greater than 530 nm for CD64 and NIMP. DAPI was excited with 360 nm and emitted at 460 nm in blue. Distinguish monocytes/macrophages and neutrophils (n = 10 images per antibody, from 3 different mice in each group) by their different labeling and count them. Express data as number of counted cells.

6. Cell Dependent Vasodilation after IRF5 Inhibition

1. Anesthetize C57Bl/6J control mice and Tsk/+ mice with and without peptide treatment with a ketamine (80 - 100 mg/kg)/xylazine (10 - 12.5 mg/kg) mixture. Inject the ketamine/xylazine mixture intraperitoneally. Restrain the mouse manually.
 1. Use a 25 gauge or smaller needle. Insert the needle into the lower right quadrant of the abdomen. Withdraw the plunger before injection to ensure that the needle does not enter a blood vessel or the bowel.
2. Once a sufficient level of anesthesia has been reached, secure the mouse in the supine position, wipe the fur with alcohol soaked gauze pad, and using a pair of scissors open the thoracic cavity and remove the heart.
NOTE: Exsanguination will euthanize the mouse and make dissection easier by relieving pressure in the vasculature thus minimizing bleeding when cutting blood vessels.
 1. Open the skin using a pair of scissors, cutting up from the chest lateral to the jawbone with care as to not disturb the underlying tissues toward the front of the jaw.
 2. Dissect the facialis artery by removing the soft tissue around it.

3. Caution: Do not injure the vessel or tug on facialis artery while keeping the exposed tissue bathed in MOPS buffer (2.0 mM $\text{CaCl}_2 \cdot 2\text{H}_2\text{O}$, 0.02 mM EDTA, 5.0 mM glucose, 4.7 mM KCl, 1.17 mM $\text{MgSO}_4 \cdot 7\text{H}_2\text{O}$, 3.0 mM MOPS, 145 mM NaCl, 1.2 mM $\text{NaH}_2\text{PO}_4 \cdot \text{H}_2\text{O}$, 2.0 mM pyruvic acid) to prevent desiccation. Perform under a binocular stereo zoom dissecting microscope (magnification of 3.5X to 45X) and a fiber optic light source.
3. Isolate the facialis artery.
 1. Grasp the facialis proximal to the first bifurcation and distal to where the artery will be cut. Cut the artery from the parent artery, the external carotid artery. Remove the facialis arteries from control mice, Tsk/+ mice with and without IRF5D treatment.
 2. While still holding the artery in the forceps, cut the two branches coming off the facialis, allowing the vessel to be gently lifted while any uncut surrounding tissue can be identified and severed.
 3. Continue this way until the bifurcation is reached cutting both daughter arteries to free the vessel. There is no need to clamp the vessels prior to cutting due to relieved pressure in the vasculature from removing the heart. Put the vessel in MOPS buffer while the other facialis artery is dissected and isolated.
 4. Cannulate the vessels by tying them onto glass pipettes with a terminal diameter of 125 - 175 μm . Preload the glass pipettes and buffer reservoirs with MOPS buffer.
Caution: Prevent air bubbles from forming in the pipettes.
 5. Tie the vessels onto the pipettes using ophthalmic sutures.
4. Mount the vessel chambers on an inverted triocular microscope with a video camera attachment. Run the video through a video caliper measurement system for on screen measurements of the vessels.²⁰
 1. Pressurize them in a two-step process. First, with the MOPS-filled reservoirs at a height above the vessel equal to 20 mmHg pressure, manually open the stopcock valves in the reservoir lines to the vessel. Inspect the vessel for signs of leaking around the ties and down the length of the vessel. Second, raise the reservoirs to 60 mmHg and reinspect the vessel.
 2. Once pressurized at 60 mmHg, allow the vessels to equilibrate for 30 min.
5. In order to assess vasodilation in response to acetylcholine (10^{-7} to 10^{-4} M), precontract the vessel to a diameter 50 - 75% of its maximum diameter using $1 - 3.0 \times 10^{-8}$ to 10^{-7} M U46619. After allowing the vessel to stabilize for 6 min, add acetylcholine to the bath in 2 min duration steps such that the final concentrations in the bath are 10^{-7} , 10^{-6} , 10^{-5} , 10^{-4} . Measure the vasodilation in all three groups.

7. Isolation of Cardiac Extracellular Matrix

1. Anesthetize C57Bl/6J control mice and Tsk/+ mice with and without peptide treatment with isoflurane (5%) and perform a cervical dislocation. Excise the hearts by cutting open the chest along the sternum. Lift up the heart with forceps and remove the heart.
2. Put the removed hearts into a beaker and add 15 mL hypertonic 1% sodium dodecyl sulfate (SDS). Agitate hearts in the 1% SDS solution for 18 h at room temperature to break up the cells by adding a stir bar to the 1% SDS solution and putting the beaker on a stir plate.
Caution: Be aware that extracellular matrix will disintegrate if left too long in hypertonic solution. Conversely, if the hearts are not agitated long enough in hypertonic solution, then the cells will not properly dissolve and there will be cell debris left in the beaker.
3. Wash for 30 min in 15 mL 0.5% Triton X-100. Then wash for 15 min with 15 mL PBS. Decellularize each heart individually.
4. Snap-freeze the extracellular matrix in liquid nitrogen and powderize the frozen cardiac extracellular matrix with a pre-cooled mortar and pestle.
5. Make a suspension of the pulverized matrix in PBS containing 1% antibiotic. The volume added in most cases is 300 μL . Sonicate the suspension for 30 - 60 s on ice on the high setting.
NOTE: It is very important that the sample keeps cold. Be aware that the suspension is very viscous due to the high protein glycan content.
6. Determine protein concentration using a Bradford assay.
NOTE: Ensure that there is anti-biotic and anti-fungal in the suspension. Penicillin/Streptomycin are the most commonly used and recommended.

8. Assessment of Nuclear Translocation by Immunohistochemistry

1. To coat dishes and slides use a final concentration of 20 $\mu\text{g}/\text{mL}$ of the cardiac extracellular matrix in PBS. Pipet 500 μL of the cardiac extracellular matrix solution into a 100 mm dish for coating and 150 μL of the final extracellular matrix solution onto a slide.
2. Inhibit IRF5 by adding IRF5D in a 50 $\mu\text{g}/\text{mL}$ concentration for 24 h to rat neonatal cardiac myocytes in culture. Leave control myocyte cultures untreated.
3. Assess trafficking of IRF5 from the cytosol to the nucleus using immunofluorescence and analyze by confocal microscopy. Identify the green labeling for IRF5, identify the blue DAPI stain for the nucleus
4. Apply the primary anti-IRF5 antibody. The primary antibody was used in a 1:200 dilution in PBS. Incubate the slides for 30 min at 37 °C and follow with three 5-min wash steps. The secondary antibody was Alexa 488-labeled goat anti-mouse IgG antibody.
5. Dilute the secondary antibody 1:1,000 dilution in PBS. Incubate the secondary antibody for 30 min at 37 °C. Achieve nuclear stain with DAPI. Dilute DAPI 1:1,000 in PBS. Wash the slides a total of 3 times for 5 min and add DAPI to the third and last wash step.
6. Capture trafficking by using confocal microscopy and measure fluorescence intensity in the nuclei and cytosol as previously described¹⁰. Identify the green labeling for IRF5, identify the blue DAPI stain for the nucleus. The cells that exhibit blue nuclei with green labeling in them contain activated IRF5, which trafficked from the cytosol to the nucleus. When IRF5 is not activated green labeling is found in the cytosol.
7. Analyze the fluorescently labeled cells by confocal microscopy using a 40X oil objective. Use an excitation wavelength of 488 nm and emission wavelengths of greater than 530 nm for IRF5. Use an excitation wavelength of 360 nm and an emission wavelength of 460 nm for visualization of DAPI.

9. Statistics

1. Perform analysis of variance (ANOVA) for repeated measures within and between groups. Follow ANOVA with Bonferroni's modification of Student's t-test. Express data as the standard error of the mean.

Representative Results

The results demonstrated in **Figure 1** show how to design a peptide. **Figure 1**, upper left, shows the region (between the 2 yellow arrows, amino acids (aa) 425-436) in IRF5 that is phosphorylated by a number of kinases. **Figure 1**, upper right, shows a yellow oval where IRF5's phosphorylated domain binds. The dimeric structure of 3DSH was rotated to observe a cleft or valley to the left of the Helix 2 (aa303-312). This is where the phospho-tail domain of IRF5 is supposed to bind when it is fully activated (*i.e.*, serine phosphorylated), forming a homodimer and its assumed biologically active state.

In **Figure 2**, the binding activity measured by biolayer interferometry is depicted. To determine that the decoy peptide IRF5D is not toxic, proliferation and apoptosis were assessed after treating the cells with increasing concentrations of IRF5D (**Figure 3**). ICAM-1, an inflammatory marker, and IRF5 expressions were reduced after treating the Tsk/+ mice with IRF5D as determined by western blot analysis (**Figure 4**). The number of neutrophils (NIMP) and CD64 were decreased as determined by immunohistochemistry after treatment with IRF5D (**Figure 5**). Endothelial function was improved in facialis arteries of Tsk/+ mice after IRF5D compared to Tsk/+ mice without IRF5D treatment (**Figure 6**). Greater numbers of IRF5 positive nuclei in myocytes cultured on Tsk/+ cardiac matrix were visualized compared to C57BL/6J cardiac matrix. Treatment of the cultures with IRF5D resulted in reduced number of IRF5 positive nuclei (**Figure 7**).

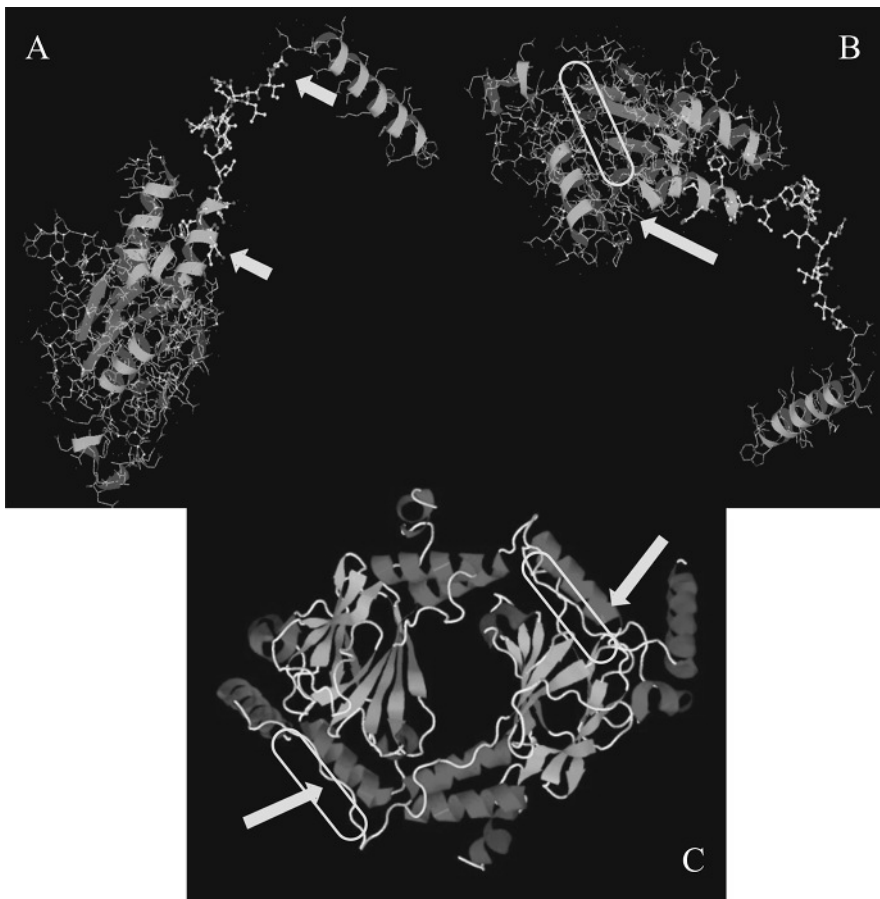


Figure 1: 3D Protein Structure of IRF5. **A)** The upper left figure shows the region the peptide was designed for. **B)** The region which is being phosphorylated highlighted by the two yellow arrows are amino acids (aa) 425 - 436 in IRF5. **C)** The lower panel depicts the homodimeric functional complex. The homodimeric figure is presented for easier viewing of the region where the phosphorylated tail domain of IRF5 binds to form a homodimer. This figure has been previously published²¹. [Please click here to view a larger version of this figure.](#)

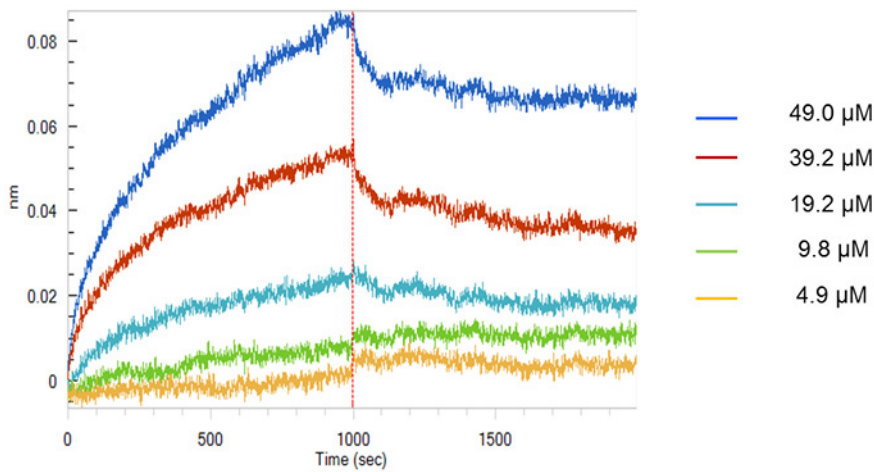


Figure 2: Bi-layer Interferometry of IRF5D. This figure shows the binding of IRF5 to IRF5D assessed by bi-layer interferometry. Analysis software showed that IRF5 binds to IRF5D with a K_d of $3.72 \pm 0.75 \times 10^{-6}$ M (mean \pm SD, $n = 3$). This figure has been previously published²¹. [Please click here to view a larger version of this figure.](#)

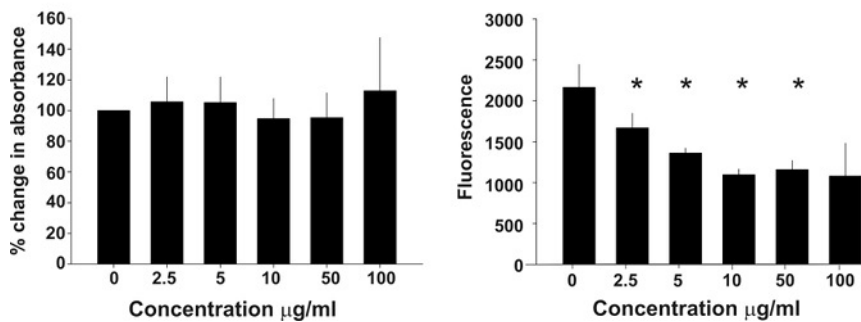


Figure 3: Cell Proliferation and Apoptosis. These bar graphs show that increasing concentrations of IRF5D have no influence on cell proliferation (left) or apoptosis (right), and were not altered by increasing levels of IRF5D. This figure has been previously published²¹ (mean \pm SD, $p < 0.05$, $n = 4$). [Please click here to view a larger version of this figure.](#)

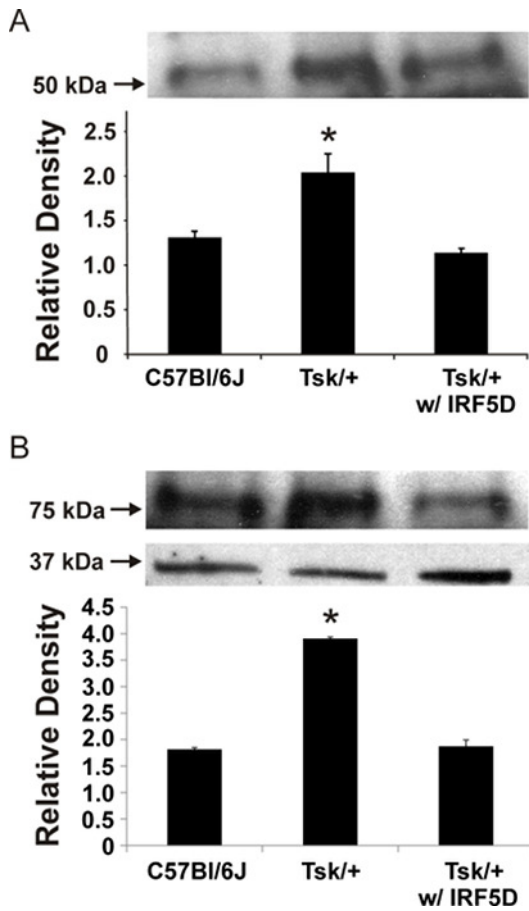


Figure 4: ICAM-1 and IRF5 Expression in the Heart. ICAM-1 (A) and IRF5 (B) expressions were decreased in the myocardium of Tsk+ mice after IRF5D treatment as demonstrated by western blot. The data was normalized to the actin loading control (mean ± SD, $p < 0.05$, $n = 3$). This figure has been previously published²¹. [Please click here to view a larger version of this figure.](#)

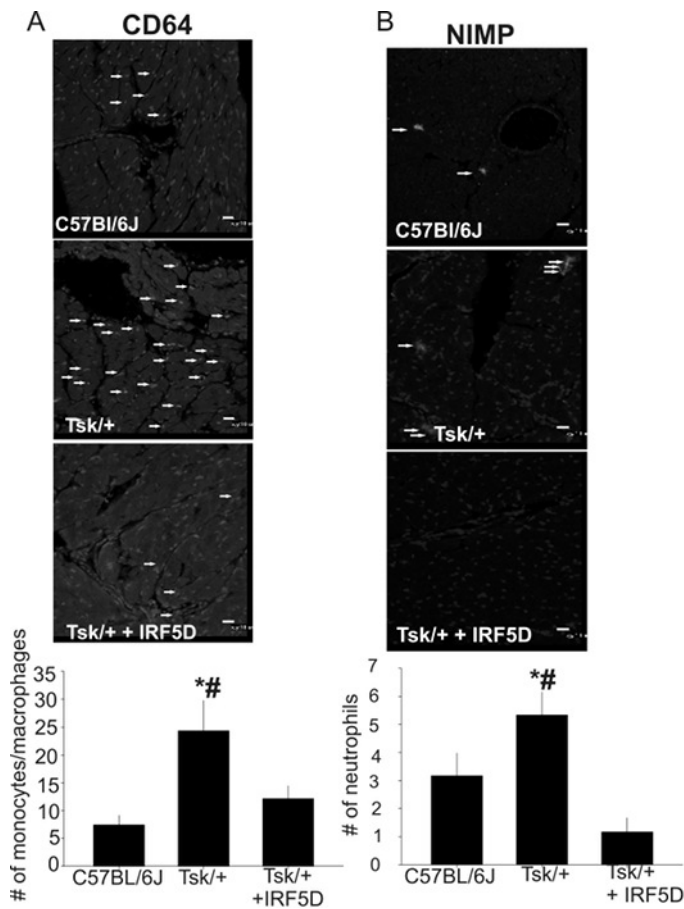


Figure 5: CD64 (A) and NIMP (B) Expression in the Heart. The number of monocytes/macrophages and neutrophils was decreased after IRF5D treatment as demonstrated by immunohistochemistry (mean \pm SD, * = $p < 0.05$, C57BL/6J vs. Tsk/+; # = $p < 0.025$, Tsk/+ vs. Tsk/+ + IRF5D; $n = 3$, 10 images per antibody). The arrows highlight monocytes/macrophages (A) and neutrophils (B). The scale bars are 10 μ m. This figure has been previously published²¹. [Please click here to view a larger version of this figure.](#)

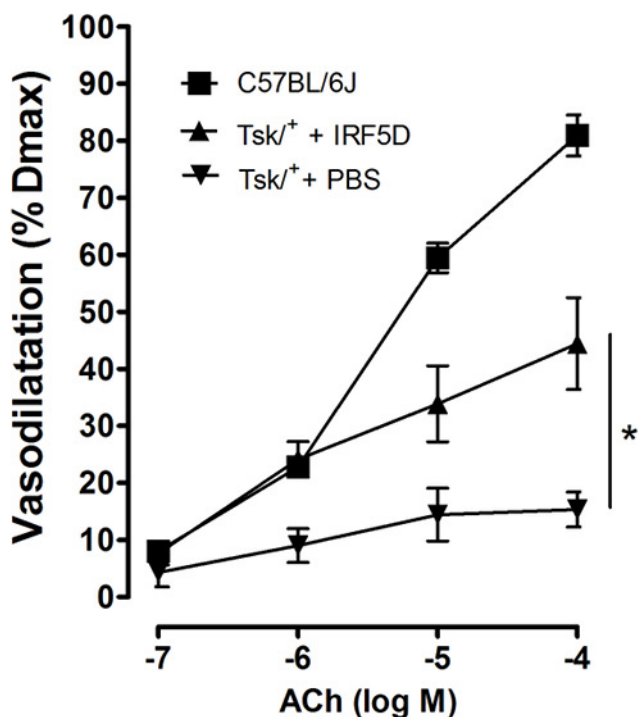


Figure 6: Cell Function and Vasodilation. IRF5D administration improved acetylcholine induced vasodilation of facialis arteries of Tsk/+ mice (mean \pm SD, $p < 0.05$, $n = 6$). This figure has been previously published²¹. [Please click here to view a larger version of this figure.](#)

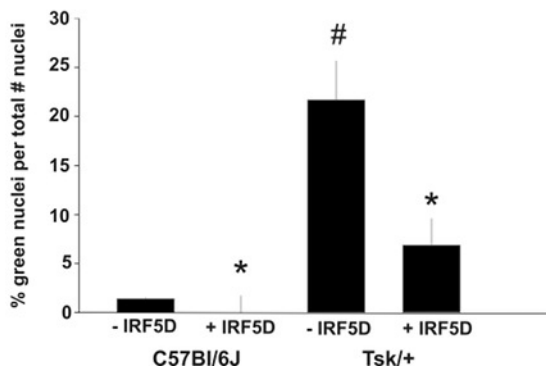
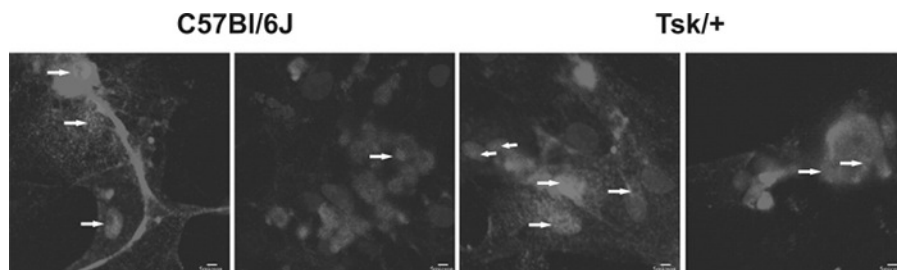


Figure 7: IRF5 Nuclear Translocation of IRF5 in Cultured Myocytes with IRF5 inhibition. IRF5 inhibition by IRF5D (50 $\mu\text{g}/\text{mL}$, 24 h) leads to fewer IRF5 positive nuclei in myocytes cultured on Tsk/+ cardiac matrix and C57BI/6J cardiac matrix. The arrows depict IRF5 positive nuclei (mean \pm SD, $p < 0.05$, $n = 3$). The scale bar is 5 μm . This figure has been previously published²¹. [Please click here to view a larger version of this figure.](#)

Discussion

The goal was to design an IRF5 inhibitor to elucidate the role of IRF5 on inflammation, fibrosis, and vascular function in the hearts of Tsk/+ mice. The findings are that IRF5D did not induce proliferation or apoptosis. Moreover, inflammation was reduced and vascular function improved.

These data suggest that IRF5 plays an important mechanistic role in the development of inflammation and fibrosis in the heart of Tsk/+ mice and that it has the potential to serve as a therapeutic target.

The first step was to design an inhibitor. When a peptide is designed, several points have to be taken into consideration: sequence length, secondary structure, residues prone to oxidation, amino acid composition, amidation and capping, amino acids in the N-terminus and amino acids in the C-terminus, and ligand attachment. The ideal sequence length is between 10 to 15 residues to ensure best overall yield, fewer impurities, and reduced cost. It is important to be aware of secondary structures like beta sheet formation. Beta sheet formation can result in a high degree of deleted sequences. Avoid residues prone to oxidation which can lead to side reactions which can impact the effectiveness of the peptide. To control solubility, synthesis, and purification, keep the composition of the amino acid building blocks for the peptide below 50% hydrophobic amino acids and ensure that there are enough charged residues. N- and C- termini need to be chosen in an uncharged state. Avoid glutamate at the N-terminus and avoid cysteine, proline, and glycine at the C-terminus. Add a spacer between the peptide and ligand to minimize folding. Therefore, they might need to be masked as an amide without charge.

IRF5D design was based on the 3D structure. A 17 mer, termed IRF5D (ELDWDADDIRLQIDNPD) was designed, where aspartate (D) was substituted for serine (S) to mimic phosphorylation in IRF5 at 421-438 (ELSWADSIRLQISNPD). This approach is straight forward due to novel computer technology. The drawback of this technique is the initial investment in the software. However, there are significant overall savings when compared with the costs associated with labor and materials used in other inhibitor design methods, like phage display²². The critical step in this process is the availability of the 3D structure of the target protein and its possible binding sites. The limitation of designing an inhibitor is the possibility that a wrong region is chosen and the inhibitor is not blocking the desired protein. The other possibility is a partial blocking of the desired protein.

With the peptide in hand the focus moves to testing the toxicity of the decoy peptide by measuring cell survival. First, IRF5D was tested using varying concentrations. IRF5D does not induce apoptosis and does not promote proliferation even at higher concentrations. The methods used here are standard and give reliable data. The tetrazolium dye bioreduction has been used for many years²³. This assay was chosen because of its reproducibility and time-effectiveness as compared to other methods, e.g., counting cells manually which is very time-consuming. Using BrdU to label proliferating cells requires radioactivity, which is sensitive, but can be hazardous. The tetrazolium dye bioreduction is time-efficient and does not require radioactivity. The limitations of the tetrazolium dye bioreduction is prevalent in studies involving oxido-reductive potential. Wherever oxido-reductive potential occurs, false positives are more frequent²⁴.

The isolation of the extracellular matrix was acquired by dissolving all myocardial cells with a hypertonic solution. The protocol was evolved from studies using a perfusion apparatus to a simple agitation process²⁵. The duration was assessed empirically by taking different time points: 12, 14, 16, 18, 20 h. The extracellular matrix was analyzed for cell debris after the different time points²⁵. The main pitfalls of decellularization are fungal and bacterial contamination. It is advised to use anti-fungal and anti-microbial compounds. To coat dishes, the extracellular matrix is powderized and suspended in PBS. Due to the high content of elastic material, the sample does not completely dissolve. Sonication on higher intensity settings without heating up the sample is imperative. The advantage of using extracellular matrix over other coating agents is that the extracellular matrix is an amalgamation of proteins physiologically occurring and it connects the *in vivo* and *in vitro* assays. This approach is more physiological than coating with a single compound like collagen or fibronectin alone. It also gives insight into the importance of signaling initiated by changes in the extracellular matrix. A limitation of this protocol is clearly the destruction of the matrix and removing important signaling components from the matrix. It is imperative to be cautious when decellularizing the matrix.

The use of intact tissue like isolated vessels opens up the possibility to study vasodilation *in situ* and with minimal interference of enzymes. This method is most adequate to study endothelial function in a variety of animals and diseases. Duling was the first to describe this method in pigs. The vessels in pig are deep in the tissue; hence the paper described the gelatin fixation. Early studies in vasodilation used carotid arteries²⁶. We refined the technique to use facialis arteries²⁷. Facialis arteries are more equivalent in size to a resistance artery than the carotid artery. A limitation of this protocol is the fragility of the vessel, which needs to be removed intact requiring practice.

In summary, developing IRF5D enabled us to assess the involvement of IRF5 in inflammation and fibrosis in the heart. This resulted in the data depicted in this study. IRF5D is a useful tool to study the mechanisms of IRF5 in various diseases as well as suggests IRF5 as a possible drug target²⁸.

Disclosures

The authors declare that they have no competing financial interests.

Acknowledgements

This work was supported by NIH grants HL-089779 (DW), HL-112270 (KAP) and HL-102836 (KAP) and Cimphoni Life Sciences (part of DW salary). The authors thank Meghann Sytsma for editing the manuscript.

References

1. Bi, X., *et al.* Loss of interferon regulatory factor 5 (IRF5) expression in human ductal carcinoma correlates with disease stage and contributes to metastasis. *Breast Cancer Res.* **13** (6), R111 (2011).
2. Dideberg, V., *et al.* An insertion-deletion polymorphism in the interferon regulatory Factor 5 (IRF5) gene confers risk of inflammatory bowel diseases. *Hum Mol Genet.* **16** (24), 3008-3016 (2007).
3. Graham, R.R., *et al.* A common haplotype of interferon regulatory factor 5 (IRF5) regulates splicing and expression and is associated with increased risk of systemic lupus erythematosus. *Nat. Genet.* **38** (5), 550-555 (2006).

4. Krausgruber, T., *et al.* IRF5 promotes inflammatory macrophage polarization and TH1-TH17 responses. *Nat. Immunol.* **12** (3), 231-238 (2011).
5. Eames, H.L., Corbin, A.L., & Udalova, I.A. Interferon regulatory factor 5 in human autoimmunity and murine models of autoimmune disease. *Transl Res.* **167** (1), 167-182 (2016).
6. Mayes, M.D., *et al.* ImmunoChIP analysis identifies multiple susceptibility Loci for systemic sclerosis. *Am J Hum Genet.* **94** (1), 47-61 (2014).
7. Dimitroulas, T., *et al.* Micro-and Macrovascular Treatment Targets in Scleroderma Heart Disease. *Curr Pharm Des.* (2013).
8. Botstein, G.R., & LeRoy, E.C. Primary heart disease in systemic sclerosis (scleroderma): advances in clinical and pathologic features, pathogenesis, and new therapeutic approaches. *Am Heart J.* **102** (5), 913-919 (1981).
9. Oram, S., & Stokes, W. The heart in scleroderma. *Br Heart J.* **23** (3), 243-259 (1961).
10. Xu, H., *et al.* 4F decreases IRF5 expression and activation in hearts of tight-skin mice. *PLoS One.* **7** (12), e52046 (2012).
11. Steen, V. The heart in systemic sclerosis. *Curr.Rheumatol.Rep.* **6** (2), 137-140 (2004).
12. Deshpande, N., *et al.* The RCSB Protein Data Bank: a redesigned query system and relational database based on the mmCIF schema. *Nucleic Acids Res.* **33** (Database issue), D233-7 (2005).
13. Concepcion, J., *et al.* Label-free detection of biomolecular interactions using biolayer interferometry for kinetic characterization. *Comb Chem High Throughput Screen.* **12** (8), 791-800 (2009).
14. Matthew, A. Current biosensor technologies in drug discovery. *Drug Discovery.* 69 (2006).
15. Doppelt-Azeroual, O., Moriaud, F., Adcock, S.A., & Delfaud, F. A review of MED-SuMo applications. *Infect Disord Drug Targets.* **9** (3), 344-357 (2009).
16. Kim, S., Jang, J., Yu, J., & Chang, J. Single mucosal immunization of recombinant adenovirus-based vaccine expressing F1 protein fragment induces protective mucosal immunity against respiratory syncytial virus infection. *Vaccine.* **28** (22), 3801-3808 (2010).
17. Frenzel, D., & Willbold, D. Kinetic Titration Series with Biolayer Interferometry. *PLoS one.* **9** (9), e106882 (2014).
18. Ou, J., *et al.* L-4F, an apolipoprotein A-1 mimetic, dramatically improves vasodilation in hypercholesterolemia and sickle cell disease. *Circulation.* **107** (18), 2337-2341 (2003).
19. Bradford, M.M. A rapid and sensitive method for the quantitation of microgram quantities of protein utilizing the principle of protein-dye binding. *Anal.Biochem.* **72** (1-2), 248-254 (1976).
20. Bauer, P.M., *et al.* Compensatory phosphorylation and protein-protein interactions revealed by loss of function and gain of function mutants of multiple serine phosphorylation sites in endothelial nitric-oxide synthase. *J.Biol.Chem.* **278** (17), 14841-14849 (2003).
21. Weihrauch, D., *et al.* An IRF5 Decoy Peptide Reduces Myocardial Inflammation and Fibrosis and Improves Endothelial Cell Function in Tight-Skin Mice. *PLoS One.* **11** (4), e0151999 (2016).
22. Hoogenboom, H.R., *et al.* Antibody phage display technology and its applications. *Immunotechnology.* **4** (1), 1-20 (1998).
23. Roehm, N.W., Rodgers, G.H., Hatfield, S.M., & Glasebrook, A.L. An improved colorimetric assay for cell proliferation and viability utilizing the tetrazolium salt XTT. *J Immunol Methods.* **142** (2), 257-265 (1991).
24. Van Tonder, A., Joubert, A.M., & Cromarty, A.D. Limitations of the 3-(4, 5-dimethylthiazol-2-yl)-2, 5-diphenyl-2H-tetrazolium bromide (MTT) assay when compared to three commonly used cell enumeration assays. *BMC Res Notes.* **8** (1), 1 (2015).
25. Ott, H.C., *et al.* Perfusion-decellularized matrix: using nature's platform to engineer a bioartificial heart. *Nat Med.* **14** (2), 213-221 (2008).
26. Ou, J., *et al.* L-4F, an apolipoprotein A-1 mimetic, dramatically improves vasodilation in hypercholesterolemia and sickle cell disease. *Circulation.* **107** (18), 2337-2341 (2003).
27. Weihrauch, D., *et al.* Effects of D-4F on vasodilation, oxidative stress, angiotensin, myocardial inflammation, and angiogenic potential in tight-skin mice. *Am J Physiol Heart Circ Physiol.* **293** (3), H1432-41 (2007).
28. Roy S, P.P. IRF-5 - A New Link to Autoimmune Diseases. In: *Autoimmune Disorders - Pathogenetic Aspects.* Mavragani, C., ed., 35 (2011).